

**DETECTION OF STRUCTURALLY BOUND HYDROXYL IN APATITE FROM APOLLO MARE BASALT 15058,128 USING TOF-SIMS.** F. M. McCubbin<sup>1</sup>, A. Steele<sup>1</sup>, H. Nekvasil<sup>2</sup>, A. Schnieders<sup>3</sup>, T. Rose<sup>4</sup>, M. Fries<sup>5</sup>, P. K. Carpenter<sup>6</sup>, and B. L. Jolliff<sup>6</sup>. <sup>1</sup> Geophysical Laboratory, Carnegie Institution of Washington, 5251 Broad Branch Rd., N.W., Washington, DC 20015. <sup>2</sup> Department of Geosciences, Stony Brook University, Stony Brook NY 11794-2100. <sup>3</sup> ION-TOF USA, Inc. 100 Red Schoolhouse Rd., Bldg. A, Chestnut Ridge, NY 10977. <sup>4</sup> Department of Mineral Sciences, National Museum of Natural History, Smithsonian Institution, Washington, DC 20560. <sup>5</sup> Jet Propulsion Laboratory, M/S 183-301, 4800 Oak Grove Drive, Pasadena, CA 91109. <sup>6</sup> Dept. of Earth and Planetary Sciences and the McDonnell Center for the Space Sciences, Washington University, Saint Louis, MO 63130. [fmccubbin@ciw.edu](mailto:fmccubbin@ciw.edu)

**Introduction:** The Moon is widely believed to be nearly devoid of indigenous magmatic water; a recent estimate of the bulk lunar water content indicated the lunar interior contains less than 1 ppb H<sub>2</sub>O [i.e., 1]. The absence of water in lunar magmas marks a stark contrast between lunar and terrestrial magmatism, especially because water has strong effects on the thermochemical and physical properties of magmas, magma transport, eruption, and degassing. While magmatic volatiles are still required to explain the lunar fire-fountains that produced pyroclastic glass deposits, carbon-species, chlorine, fluorine, and sulfur are typically implicated as the propellants [i.e., 2, 3-5]. Recent evidence, however, indicates that some lunar magmas may have contained more water than previously estimated. Saal et al. [6] reported finding up to 46 ppm H<sub>2</sub>O in the cores of some lunar volcanic glass beads analyzed by secondary ion mass spectrometry. This work represents the first report of magmatic water in lunar materials, but prior to the work presented here, indigenous water has not been directly detected in lunar magmatic minerals [e.g., 7].

On Earth, a variety of minerals contain water as an essential structural constituent (ESC) such as clays, hydroxides, micas, amphiboles, and many phosphates and sulfates. However, with the exception of apatite, these minerals have not been discovered in lunar samples. The mineral apatite [Ca<sub>5</sub>(PO<sub>4</sub>)<sub>3</sub>(F,Cl,OH)] is one of the primary mineralogical reservoirs for phosphorus on Earth and it is a ubiquitous (albeit trace) phase in many lunar rocks. Lunar apatite has never been analyzed directly for water and has almost exclusively been referred to as F-Cl apatite either because measured F-Cl sums are very close to stoichiometrically filling the monovalent anion site (X-site) or based on the notion that water did not exist in lunar magmas. Moreover, nominally anhydrous RE-merrillite occurs in lunar rocks instead of H-bearing whitlockite, which is the stable form of this mineral on Earth [8-10]. Recently, however, high-quality electron microprobe analyses have indicated crystal chemical evidence for a missing component in the X-site of some lunar apatites [11]. This observation points to the possibility that OH<sup>-</sup> is present within lunar apatite. In this study, we have analyzed lunar apatite from an Apollo 15 Mare basalt

(15058,128) using time-of-flight secondary ion mass spectrometry (TOF-SIMS), Raman spectral imaging, Raman spectroscopy, electron probe microanalysis (EPMA), and field emission scanning electron microscopy (FE-SEM) to answer this question.

**TOF-SIMS Instrument:** TOF-SIMS analysis was performed using a TOF-SIMS IV instrument from Ion-TOF GmbH housed in the Department of Mineral Sciences at the Smithsonian Institution in Washington DC. TOF-SIMS is a surface-sensitive analysis method, and the information depth is only one to three atomic monolayers. As a result, sputter cleaning was performed on each of our analysis targets until a baseline number of counts was reached for a host of common surface contaminants. Approximately two minutes of sputtering with a 3 keV Ar<sup>+</sup> ion beam at 30 nA of current on a 300 x 300 μm<sup>2</sup> area was required for each analysis target.

During sample analysis, an intermittent Bi<sup>+</sup> primary ion beam with a pulse length of ~1 ns was used. The mass resolution for this technique is ~5000 at mass 17 amu, which is sensitive enough to discriminate between <sup>16,999</sup>[O]<sup>-</sup> and <sup>17,003</sup>[OH]<sup>-</sup>. Spectra were collected in negative and positive ion mode. Mass calibration was performed from these spectra using the system reference masses at m/z 1.008 [H]<sup>-</sup>, m/z 12.000 [C]<sup>-</sup>, m/z 13.008 [CH]<sup>-</sup>, m/z 14.016 [CH<sub>2</sub>]<sup>-</sup>, and m/z 15.023 [CH<sub>3</sub>]<sup>-</sup> for negative ions and m/z 15.023 [CH<sub>3</sub>]<sup>+</sup>, m/z 29.039 [C<sub>2</sub>H<sub>5</sub>]<sup>+</sup>, and m/z 43.055 [C<sub>3</sub>H<sub>7</sub>]<sup>+</sup>, for positive ions. The same target areas were then reanalyzed using a pulse length of ~100 ns, which was necessary to obtain high lateral-resolution ion images. For image acquisition, the analyzed sample regions were raster-scanned with 256<sup>2</sup> pixels, using 1 shot per pixel in each scan. Each measurement consisted of ~50-150 scans, dependent on total ion yield, corresponding to total measurement times of ~10-20 minutes. Further details of the TOF-SIMS technique is given by Stephan [12].

**TOF-SIMS Analysis:** Two apatite-rich regions (each ~55 μm x 55 μm) within 15058,128 were imaged with the TOF-SIMS instrument. The resulting images are presented in Figure 1. The <sup>18,998</sup>[F]<sup>-</sup>, <sup>34,969</sup>[Cl]<sup>-</sup>, and <sup>17,003</sup>[OH]<sup>-</sup> ion-images (collected by TOF-SIMS) in Figure 1a correlate nearly 1:1 with apatite (verified by Raman spectral imaging). The <sup>18,998</sup>[F]<sup>-</sup> and <sup>17,003</sup>[OH]<sup>-</sup>

TOF-SIMS images in Figure 1b also correlate nearly 1:1 with apatite, however the  $^{34,969}\text{[Cl]}^-$  image in Figure 1b shows very low intensity across the entire imaged region, although it still shows a positive correlation with the apatite, consistent with apatite being the primary host for chlorine.

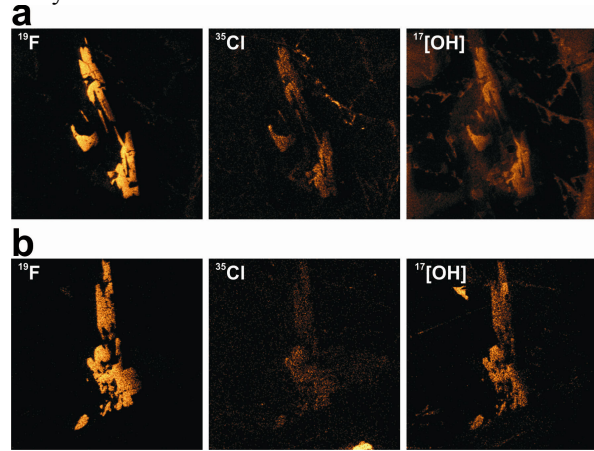


Figure 1. TOF-SIMS ion images collected from the two apatite-bearing analysis targets. Each image is labeled with the chemical constituent that is being imaged. The field of view for all of the images is about  $210\mu\text{m} \times 210\mu\text{m}$ . a) The three images in this section are from analysis target 1. b) The three images in this section are from analysis target 2.

**EPMA Analysis:** Apatite in 15058 is predominantly fluorapatite, with chlorapatite components ranging from about 1 to 7 mol.%. Apatite grain sizes ranged from 5 to 30 micrometers and grain shapes are commonly subhedral to anhedral and dictated by the interstitial spaces in which late-stage mesostasis crystallized. Most of the phosphate in 15058,128 is apatite, although we found one grain of RE-merrillite during the course of our analyses

Apatite analyses from 15058,128 had an average  $\text{F}+\text{Cl}$  sum of  $0.980 \pm 0.064$  (standard deviation) when normalized to 13 anions (i.e., 25 negative charges), which is within error of 1.00sfu or stoichiometric filling of the apatite X-site. However, some individual analyses yielded  $\text{F}+\text{Cl}$  sums that are less than 1.00 by an amount that exceeds the analytical uncertainty, and we use these analyses to set an upper limit on the amount of  $\text{OH}^-$  that could be present. The lowest measured fluorine value is 2.99 wt.%. This fluorine concentration and the accompanying chlorine correspond to a  $\text{F}+\text{Cl}$  sum of  $0.864 \pm 0.059$  atoms per formula unit. These values set an upper limit on  $\text{OH}^-$  concentration of about  $4600 \pm 2000$  ppm or  $270 \pm 120$  ppm H (equivalent to about  $2400 \pm 1100$  ppm  $\text{H}_2\text{O}$ ). Volatile contents of apatite from 15058,128 are presented in Figure 2.

**Conclusions:** The TOF-SIMS data show that  $\text{OH}^-$  is present in apatite from mare basalt 15058,128. This is the first direct evidence of structurally bound water in a lunar magmatic mineral. Although quantification

of the water content of the apatite is not possible from these data, some constraints on the  $\text{OH}^-$  content of the apatite can be made based on the missing components in the apatite X-site from EPMA data. Although many of the analyses fell within the uncertainty of detecting a missing component in the apatite X-site (0.07 apfu or 1250 ppm  $\text{H}_2\text{O}$ ), the upper limit on possible  $\text{OH}^-$  contents for the apatite in 15058,128 from EPMA data is  $4600 \pm 2000$  ppm (i.e.,  $2400 \pm 1100$  ppm  $\text{H}_2\text{O}$ ). As quantitative measurement of water becomes possible through the availability of apatite standards for dynamic SIMS measurements, the precise water contents of lunar apatites will be determined. However, the TOF-SIMS data provides evidence that there is at least some hydroxyl in a number of apatite grains from 15058,128. Furthermore, these results lend support to the assignment of at least some of the missing structural component in the monovalent anion site (X-site) of other lunar apatites, especially those in mare basalts, to  $\text{OH}^-$

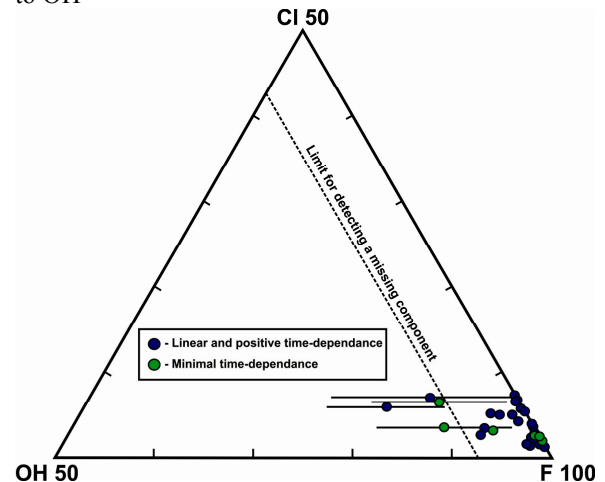


Figure 2. Truncated ternary plot of apatite X-site occupancy (mol%) from 15058, 128. Data yielding  $(\text{F} + \text{Cl}) > 1$  atom are plotted along the  $\text{OH}^-$  free join assuming  $1 - \text{Cl} = \text{F}$ . Analyses that exhibited fluorine count time-dependence during electron microprobe (EMP) analysis are shown in blue; those with minimal count acceleration are in green. The dashed line represents the average uncertainty on the fluorine value, which is equivalent to about 0.07 apfu. Error bars are present for analyses that plotted outside of the missing component detection limit field.

**References:** [1] S. R. Taylor et al., (2006) *New Views of the Moon* **60**, 657. [2] R. O. Colson (1992) *Proc. LPSC 22* 427-436 [3] L. T. Elkins-Tanton et al. (2003) *GRL* **30** [4] R. A. Fogel, M. J. Rutherford, *GCA* **59**, 201 (1995). [5] M. J. Rutherford & P. Papale (2009) *Geology* **37**, 219-222 [6] A. E. Saal et al., *Nature* **454**, 192 (2008). [7] A.H. Treiman (2008) *Am Min.* **93**, 488-491. [8] J. M. Hughes et al. (2006) *Am. Min.* **91**, 1547-1552 [9] (2008) J. M. Hughes et al. *Am Min.* **93**, 1300-1305. [10] B. L. Jolliff et al., *Am Min* **91**, 1583 (2006). [11] F. M. McCubbin & H. Nekvasil (2009) *GCA* **73**, A855. [12] T. Stephan (2001) *Planet. & Space Sci.* **49**, 859-906.